Journal of Cellular Biochemistry 79:542–556 (2000)

Taxol Reduces Cytosolic E-Cadherin and β-Catenin Levels in Nasopharyngeal Carcinoma Cell Line TW-039: Cross-Talk Between the Microtubule- and Actin-Based Cytoskeletons

Pei-Jen Lou,[1,2] Wen-Pin Chen,[1] Chin-Tarng Lin,[3] Hui-Chin Chen,[2] and Jiahn-Chun Wu[1]*

[1]Department of Anatomy and Cell Biology, College of Medicine, National Taiwan University, Taipei, Taiwan
[2]Department of Otolaryngology, National Taiwan University Hospital, Taipei, Taiwan
[3]Department of Pathology, College of Medicine, National Taiwan University, Taipei, Taiwan

Abstract Taxol affects microtubule dynamics by promoting microtubule assembly. To obtain a better insight into possible cross-talk between the microtubule- and actin-based cytoskeletons, we studied the short-term effects of Taxol treatment on the expression of actin and the E-cadherin/catenin complex in the nasopharyngeal carcinoma cell line TW-039 using immunofluorescence, immunoprecipitation, and immunoblotting methods. Morphologic changes in actin filaments, including ventral actin clumps and perijunctional actin blebs, were seen at Taxol concentrations ≥1 μM. Levels of detergent-soluble E-cadherin fell to 53% or 58% compared to controls in cells treated, respectively, with 1 or 5 μM Taxol, while levels of detergent-soluble β-catenin fell to 76% or 74%. Levels of the detergent-soluble pool of α- and γ-catenin and the detergent-insoluble pool of the E-cadherin/catenin complex were unchanged by Taxol treatment and no significant difference was seen in the levels of adenomatous polyposis coli or glycogen synthase-3β or tyrosine phosphorylation patterns. These results suggest that modulation of microtubule dynamics by Taxol may have effects on the expression of actin and the cytosolic E-cadherin and β-catenin in nasopharyngeal carcinoma cells through pathways not involving the phosphorylation of β-catenin. J. Cell. Biochem. 79:542–556, 2000.

Key words: Taxol; microtubule; actin; E-cadherin; catenin; nasopharyngeal carcinoma

Microtubules and actin filaments are cytoskeleton proteins that play crucial roles in cell growth and division, motility, signaling, and the development and maintenance of cell shape. These cytoskeletal proteins are the targets of a growing number of anti-cancer drugs [reviewed in Jordan and Wilson, 1998]. Paclitaxel (formulated as Taxol) is extracted from the bark of the Pacific yew tree, *Taxus brevifolia*, and from the needles and stems of this, and other, *Taxus* species [Schief et al., 1979]. The mechanism of action of Taxol on microtubule assembly/disassembly has been largely elucidated by Manfredi and Horwitz [1984]. In vitro, Taxol promotes microtubule assembly and binds preferentially to microtubules rather than to tubulin dimers. It reduces the critical concentration of tubulin required for polymerization. Taxol-treated microtubules are stable and resistant to disassembly, even after treatment with calcium or low temperatures, both of which usually promote this process [Manfredi and Horwitz, 1984]. Cells exposed to Taxol exhibit two distinct patterns of cellular microtubules, either abundant arrays of disorganized microtubules arranged in parallel "bundles," or abnormal mitotic asters that do not require centrioles to form [Garcia et al., 1994]. Disruption of microtubule function blocks cell-cycle progression in many cells at the prometaphase/metaphase to anaphase transition—the mitotic checkpoint. Intact cells treated with Taxol accumulate in the G2 and M phases of the cell

Grant sponsor: National Science Council of the Republic of China; Grant number: NSC 89-2314-B-002-237 and NSC-89-2314-B-002-121.

*Correspondence to: Jiahn-Chun Wu, Department of Anatomy and Cell Biology, College of Medicine, National Taiwan University, Jen-Ai Road, Taipei 10018, Taiwan. Email: jcwu@ha.mc.ntu.edu.tw

Received 28 March 2000; Accepted 5 June 2000

cycle, and the progression of mitotic cells to G1 phase is also inhibited after Taxol treatment [Long and Fairchild, 1994]. Mitotic block persists for varying lengths of time, depending on the cell type, though most cells ultimately exit mitosis and undergo apoptosis [Jordan et al., 1996; Woods et al., 1995]. In addition, Taxol appears to induce a temporary G1 block in nontransformed cells, whereas transformed cells are not blocked and undergo apoptosis [Trielli et al., 1996].

E-cadherin is a Ca^{2+}-dependent transmembrane glycoprotein responsible for establishing physical cell-cell associations and is important in tissue morphogenesis, cell polarity, and tumor invasiveness [Takeichi, 1991; Mareel et al., 1997]. Through its association with the catenins, E-cadherin is indirectly linked to the actin-based cytoskeleton, and the linkage between E-cadherin and actin filaments is required for the functional integrity of E-cadherin [Tsukita et al., 1992]. Among the catenins, β-catenin directly binds to the cytoplasmic region of E-cadherin and is responsible for homeostasis of the E-cadherin/catenin complex. The activities of β-catenin are controlled by three types of interactions: in the adherens junction, where it binds to cadherins, linking them to the actin cytoskeleton; in the nucleus, where it binds to transcriptional factors and stimulates gene expression; and in the cytoplasm, where free cytoplasmic β-catenin interacts with axin and adenomatous polyposis coli (APC) protein, which target it for degradation [reviewed in Ben-Ze'ev and Geiger, 1998]. The cellular levels of β-catenin are constitutively down-regulated by a component of the Wnt signaling pathway, glycogen synthase kinase (GSK) 3β. APC protein can form complexes with GSK, β-catenin, and possibly other members of the axin family. Nathke and colleagues [1996] showed that APC protein is localized in punctate clusters near the ends of microtubules that protrude into actively migrating membrane structures. Phosphorylation of APC and β-catenin is involved in their reciprocal interaction and in the degradation of β-catenin [Rubinfeld et al., 1996].

Cross-talk between the microtubule-based and actin-based cytoskeletons is an interesting issue. It was not until the last decade that it was clearly shown that these two cytoskeletal systems are closely associated. Yap and colleagues [1995] demonstrated that the continuous staining patterns of ZO-1 and E-cadherin in cell-cell junctions are disrupted following administration of the microtubule-depolymerizing agent, colchicine, raising the possibility that modulation of microtubules might have effects on the actin-based cytoskeleton and junctional complexes. Because β-catenin is known to be a component of both microtubule-based and actin-based complexes and to be important in maintaining the homeostasis of the E-cadherin/catenin/actin complex, we postulated that modulation of microtubules by Taxol might have effects on the E-cadherin/catenin/actin complex. In the present study, we used immunofluorescence microscopy, immunoprecipitation, and immunoblot analyses to examine the short-term effect of Taxol treatment on the distribution and expression of the E-cadherin/catenin/actin complex in a nasopharyngeal carcinoma (NPC) cell line, TW-039 [Lou et al., 2000]. The results show that, at high concentrations ($\geq$ 1 μM), Taxol reduces the detergent-soluble pools of E-cadherin and β-catenin. Morphologic changes in actin filaments are also noted at these high concentrations. In contrast, the detergent-insoluble pool of the E-cadherin/catenin complex is unaffected by Taxol treatment.

MATERIALS AND METHODS

Cell Culture

The NPC cell line, TW-039 [Lin et al., 1990], was maintained at a low cell density and grown in Dulbecco's modified Eagle's medium (DMEM) containing 1.8 mM Ca^{2+} and 10% fetal calf serum (FCS) (high calcium medium, HCM) in a 5% CO_2 incubator at 37°C. Cells at confluent density (1×10^6 cells/cm^2) were plated on coverslips in 35-mm Petri dishes or 25-cm^2 flasks (Costar, Corning, NY) and grown in DMEM containing 5 μM Ca^{2+} and 10% FCS (low calcium medium, LCM) for the subsequent Taxol treatment. Cells grown on coverslips were processed for immunofluorescence microscopy, while those grown in flasks were used in immunoprecipitation and immunoblotting studies. All the data presented were obtained from at least three independent experiments.

Antibodies

Mouse monoclonal antibodies against E-cadherin (C20820) or β-catenin (C19220) were purchased from Transduction Laboratories (Lexington, KY). Rabbit anti-β-catenin (C-2206) and anti-α-catenin (C-2801) antisera, mouse monoclonal antibodies against plakoglo-

bin (γ-catenin; P-8087), phosphoserine (P-3430), or phosphotyrosine (P-3300), and TRITC-conjugated phalloidin were purchased from Sigma (St. Louis, MO). Mouse monoclonal antibodies against APC, GSK-3, or β-tubulin were purchased, respectively, from Oncogene (Cambridge, MA), Upstate Biotechnology (Lake Placid, NY), and the Developmental Studies Hybridoma Bank (Iowa City, IA).

Taxol Treatment of Cells

Cells to be treated with Taxol were cultured in LCM for 24–36 h, then various concentrations of Taxol [Sigma; 0.1–10 μM in dimethyl sulfoxide (DMSO)] were added as a pretreatment. After 30 min, the LCM was replaced with HCM containing the same concentration of Taxol as that used for pretreatment, and incubation continued for another 2 h. The cells were then harvested for testing. Control cells were treated with DMSO and processed in the same way as the Taxol-treated cells.

Cell Viability Assay

Triplicate cell cultures were grown on 96-well plates (2,000 cells/well) in LCM for 24–36 h prior to Taxol addition. The protocol for Taxol treatment was the same as that described above. After treatment, the Taxol-containing HCM was completely removed by washing with DMEM. Fifty microliters of 3-(4,5-dimethyltiazol-2-yl)-2,5-diphenyltetrazolium bromide (MTT; Sigma), dissolved in DMEM (2 mg/ml) and filter-sterilized, was then added to each well [Twentyman and Luscombe, 1987; Carmichael et al., 1987]. After a further 4 h incubation period, the medium was aspirated as completely as possible without disturbing the formazan crystals and cells on the plastic surface. Then, 200 μl of DMSO was added to each well and the plates were shaken on a plate shaker for 5 min before the optical density at 540 nm was read using a scanning multiwell enzyme-linked immunosorbent assay reader (Microplate Autoreader EL311, Bio-Tek Instruments Inc., Winooski, VT).

Immunocytochemistry

Immunofluorescence staining was performed as described previously [Lou et al., 2000], with slight modification. All antibody reactions were at 37°C, while all other manipulations were at room temperature. Cells grown on coverslips were washed briefly in phosphate-buffered saline (PBS), then fixed in methanol or 10% formalin. After a PBS wash, the cells were incubated for 2 h with primary antibodies. After thorough washing, bound primary antibodies were visualized by incubation for 1 h at 37°C with species-specific FITC- or Texas red-conjugated secondary antibodies (Vector, Burlingame, CA). The cells were then extensively washed, mounted on a slide using PBS containing 2% n-propyl gallate and 60% glycerol, pH 8.0, sealed with nail polish, viewed using a Zeiss Axiophot microscope (Carl Zeiss, Oberkocheu, Germany) equipped with epifluorescence, and photographed using Kodak T-Max 400 film.

Detergent Extraction of Cells

Cells plated on 25-cm^2 flasks were processed for Taxol treatment as above. They were then washed three times with ice-cold CSK buffer (50 mM NaCl, 10 mM Pipes, 3 mM $MgCl_2$, 300 mM sucrose, 1.2 mM PMSF, 10 μg/ml of leupeptin, pH 6.8), transferred into an Eppendorf microtube by scraping with a cell scraper, then centrifuged at 14,000*g* for 5 min. The supernatant was discarded and 100 μl of 0.5% Triton X-100 (TX-100) in CSK buffer was added to the pellet, then the samples were incubated for 10 min with gentle pipetting before being centrifuged at 14,000*g* for 30 min. Sample buffer (2X Laemmli) was added to the supernatant to a total volume of 250 μl; this was then used as the detergent-soluble fraction, and the pellet was dissolved in 250 μl of 1X Laemmli sample buffer and used as the detergent-insoluble fraction [Lou et al., 2000; Pasdar and Nelson, 1988]. Both fractions were then subjected to 10% sodium dodecylsulfate-polyacrylamide gel electrophoresis (SDS-PAGE) and processed for immunoblotting.

Immunoprecipitation

Immunoprecipitation was performed as described previously [Lou et al., 2000]. Control and Taxol-treated cells in 25-cm^2 flasks were washed three times with ice-cold PBS, then each flask was extracted for 30 min at 0°C with 1 ml of detergent solution (10 mM Tris-HCl, pH 7.5, 0.5% NP-40, 1 mM EDTA, and 1 mM PMSF). Insoluble material was removed by centrifugation at 12,000*g* for 10 min. The supernatant was transferred to a new microtube and mixed with 2 μg of monoclonal anti-β-catenin or anti-APC antibody at 4°C. After 1 h,

100 μl of protein G-sepharose bead slurry (50 μl of packed beads; Pharmacia, Uppsala, Sweden) was added and mixing continued for a further 30 min at 4°C, then the sepharose-bound immune complexes were collected by centrifugation at 14,000*g* for 1 min at 4°C. The beads were then washed five times with detergent solution, the pellets boiled in Laemmli sample buffer for 5 min at 95°C, and the supernatant collected and processed for SDS-PAGE.

Immunoblotting

Proteins from cell extracts or immunoprecipitates were separated on SDS-PAGE and transferred electrophoretically to PROTRANE BA85 nitrocellulose membranes (Schleicher & Schuell Inc., Keene, NH). The membranes were blocked with 5% skimmed milk and the proteins of interest detected using specific monoclonal or polyclonal antibodies as indicated, followed by alkaline phosphatase-conjugated goat anti-rabbit or anti-mouse IgG (Promega, Madison, WI), as appropriate. Immunoreactive bands were visualized by substrate development using nitro blue tetrazolium and 5-bromo-4-chloro-3-indolyl phosphate. Quantification of staining was by densitometry (IS-1000 Digital Imaging System).

RESULTS

TW-039 cells were rendered contact naïve by consecutive platings at low density (Fig. 1A). The cells were then plated at confluent density in LCM for 24–36 h and incubated in the presence of various concentrations of Taxol for a further 30 min as a pretreatment. Cell-cell contacts were then synchronously induced by switching the medium to Taxol-containing HCM for 2 h, after which the cells were harvested for testing.

MTT Colorimetric Cell Viability Assay

To evaluate the short-term effects of Taxol treatment on the expression of the E-cadherin/catenin/actin complex, it was important to determine an optimal concentration of Taxol that would not affect the viability of TW-039 cells using the present experiment protocol. We therefore used the MTT colorimetric cell viability assay, a valid and simple method of assessing chemosensitivity in established cell lines [Carmichael et al., 1987], to assess the viability of TW-039 cells treated with different concentrations of Taxol. As shown in Figure 1B, cell viability was not affected by concentrations of Taxol ≤5 μM. Concentrations of 0.1, 1, and 5 μM were selected for further experiments.

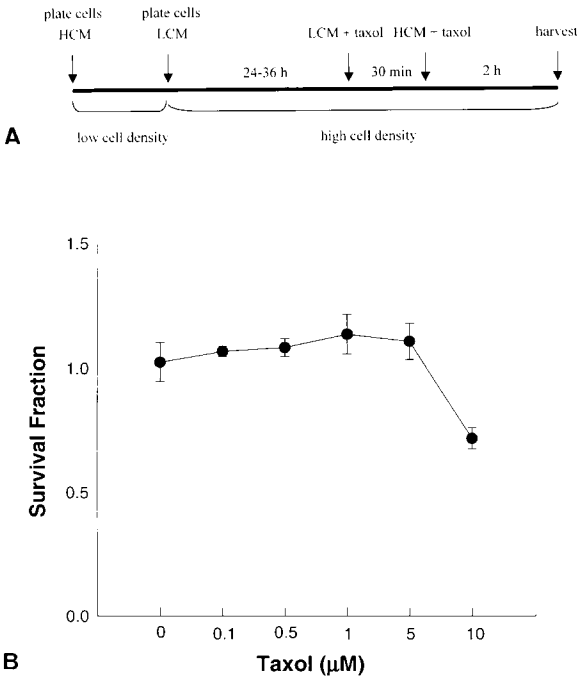

Fig. 1. Dose-dependent effects of Taxol on viability of nasopharyngeal carcinoma cell line TW-039. TW-039 cells were rendered contact naïve by consecutive platings at low density. The cells were plated at confluent density in low calcium medium for 24–36 h, incubated with different concentrations of Taxol for 30 min as a pretreatment, then placed in a Taxol-containing high calcium medium for another 2 h as outlined in the schematic time line (**A**). **B**: Viability of TW-039 cells after treatment with different concentrations of Taxol. The error bars represent the coefficient of variation for results obtained from triplicate wells. The x axis represents the Taxol concentrations. The y axis represents the surviving fraction of TW-039 cells as determined by MTT assay.

High Concentrations of Taxol Induce Rounding-Up of TW-039 Cells

In living cells, cytoskeleton proteins are important in maintaining cell shape. To investigate the influence of microtubule modulation on the actin-based cytoskeleton complex, we examined the effect of Taxol on epithelial morphology and actin expression in confluent TW-039 monolayers. No significant morphologic difference was found between control cells and cells treated with a low concentration (0.1 μM) of Taxol (Fig. 2A–2D). In contrast, exposure to high concentrations (1 and 5 μM) of Taxol induced striking morphologic changes in mono-

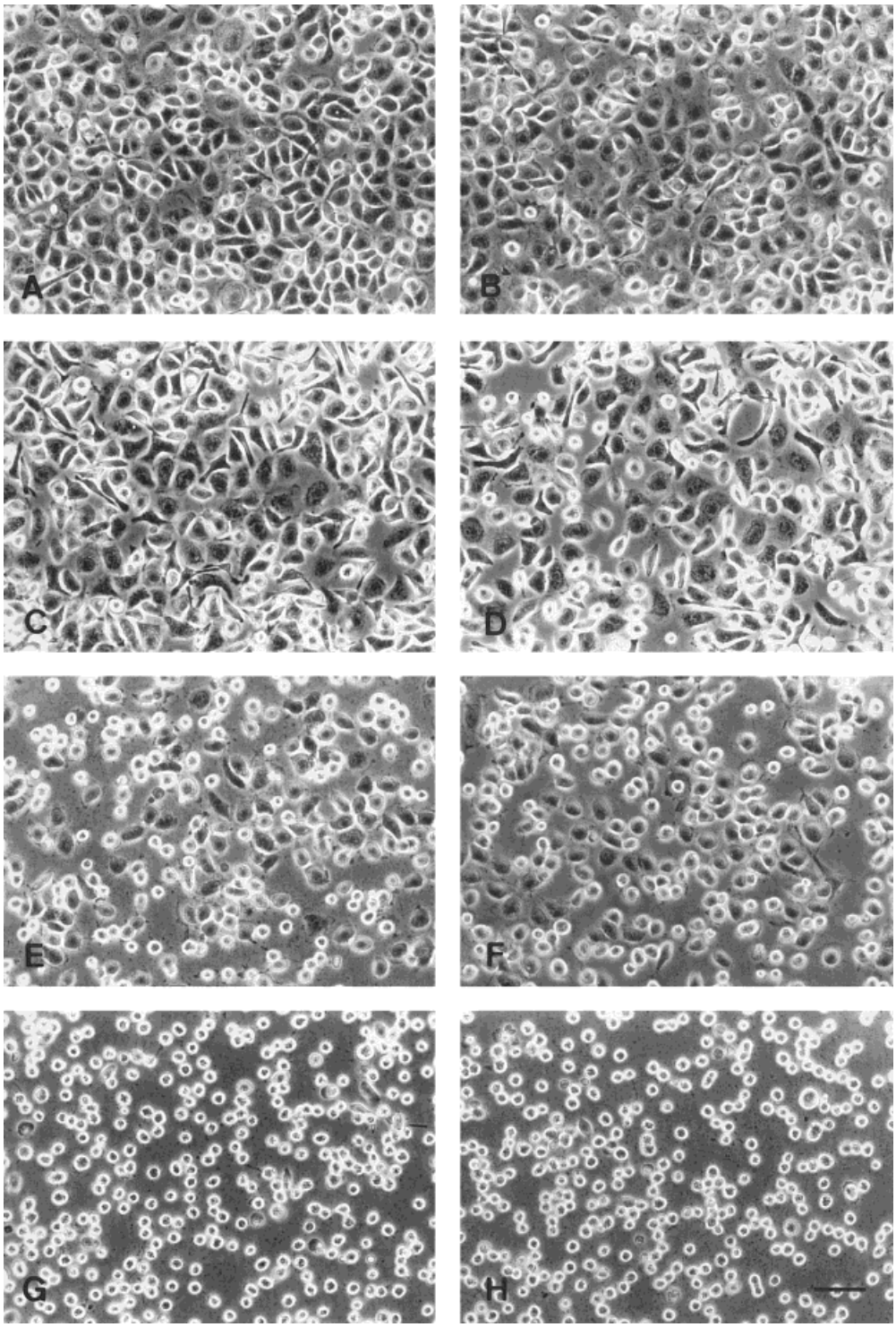

Fig. 2. Phase contrast microscopy showing Taxol-induced morphologic changes in TW-039 cells. TW-039 cells were plated at confluent density in low calcium medium for 24–36 h (**A**) as outlined in Fig. 1A and were then incubated with different concentrations of Taxol for 30 min as a pretreatment. **C**, **E**, and **G** represent cells treated with 0.1, 1, or 5 μM Taxol, respectively, after the pretreatment. **B**, **D**, **F**, and **H** represent cells treated with 0, 0.1, 1, and 5 μM of Taxol, respectively, 2 h after calcium elevation. Bar = 50 μm.

layer organization (Fig. 2E–2H). Reduction of the cell areas was seen in cells treated with 1 μM Taxol (Fig. 2E and 2F) and further rounding-up of cells is seen with 5 μM Taxol (Fig. 2G and 2H).

Effect of Taxol on Microtubule Architecture and APC Distribution

Previous studies have demonstrated that different microtubular arrangements are seen in different cell lines following treatment with taxoids: microtubular bundles being seen in interphase cells and asters in mitotic cells [Garcia et al., 1994]. In the present study, control cells exhibited delicate arrays of microtubules throughout the cytoplasm (Fig. 3A). When cells were cultured in the presence of Taxol, the microtubules became markedly disrupted (Fig. 3C, 3E, 3G). Taxol at both low (0.1 μM) and high (1 μM) concentrations induced the formation of large microtubule bundles (Fig. 3C, 3E). At an even higher concentration (5 μM), Taxol disrupted the microtubular networks, resulting in discrete filamentous segments (Fig. 3G). However, using the present experimental protocol, the microtubular asters noted in other studies were not seen. In TW-039 cells, the APC protein exhibited a diffuse cytosolic punctuate staining that did not show marked changes after Taxol treatment (Fig. 3B, 3D, 3F, 3H).

Effect of Taxol on the Distribution of Actin Filaments

Because high concentrations (1 and 5 μM) of Taxol induced rounding-up of TW-039 cells, it was important to check the effect of Taxol on the distribution of actin, a major cytoskeleton protein involved in maintaining cell shape. In control (Fig. 4A) and 0.1 μM Taxol-treated (Fig. 4C) cells, actin bundles formed stress fibers that traversed the ventral cell-substratum interfaces. In the focal plane of the cell-cell contacts, cortical actin was seen to be concentrated at perijunctional areas, exhibiting a typical honeycomb pattern in both control (Fig. 4B) and 0.1 μM Taxol-treated (Fig. 4D) cells. In marked contrast, when the Taxol concentration was increased to 1 μM, the ventral stress fibers were disrupted into large aggregates of actin clumps (Fig. 4E), and intercellular space widening and perijunctional actin blebs were also noted (Fig. 4F). At an even higher concentration (5 μM) of Taxol, the actin clumps became smaller and more dispersed (Fig. 4G); the cortical actin still encircled the cells, although the cell areas were clearly reduced (Fig. 4H).

Immunocytochemical Staining of the E-cadherin, α-, β-, and γ-Catenin Complex in Taxol-Treated TW-039 Cells

Isolated epithelial cells commonly contain large intracellular pools of E-cadherin and catenins that appear to be recruited to the cell surface following cell-cell contact. Madin-Darby canine kidney (MDCK) cells do not form cell-cell contacts in growth media containing low calcium (5 μM) because the calcium-dependent cadherin molecule is inactivated [Pasdar and Nelson, 1988]. Similar results were seen in TW-039 cells in the present study. After 24-h incubation in LCM, the distribution of E-cadherin remained cytosolic and no junctional staining was seen (Fig. 5). Two hours after transfer to HCM, both E-cadherin and the catenins were recruited to cell-cell contact sites, while still maintaining a cytosolic distribution (Fig. 6A, 6E, 6I, 6M). These calcium-induced cell-cell contacts were not affected by treatment with a low concentration of Taxol (Fig. 6B, 6F, 6J, 6N). However, when the Taxol concentration was increased, the cells rounded-up and became separated from one another (Fig. 6C, 6D, 6G, 6H, 6K, 6L, 6O, 6P), and E-cadherin (Fig. 6C, 6D) and the catenins (Fig. 6G, 6H, 6K, 6L, 6O, 6P) became concentrated at the cell-membrane and cell-cell contact sites.

Taxol Reduces the Detergent-Soluble Pools of E-Cadherin and β-Catenin

To further investigate the quantitative changes in the E-cadherin/catenin complex, we performed immunoblot and subsequent densitometric analyses. Equivalent aliquots of proteins from whole cell lysates of TW-039 cells were separated on polyacrylamide gels, transblotted, and probed with antibodies specific for E-cadherin or α-, β-, or γ-catenin. In cells treated with high concentrations (1 or 5 μM) of Taxol, there was reduced expression of E-cadherin and β-catenin, but no change in the expression of α- and γ-catenin (data not shown). It is well documented that, in living cells, E-cadherin and the catenins are present in two separate pools, with the cytoskeleton-bound cadherin/catenin complex being resis-

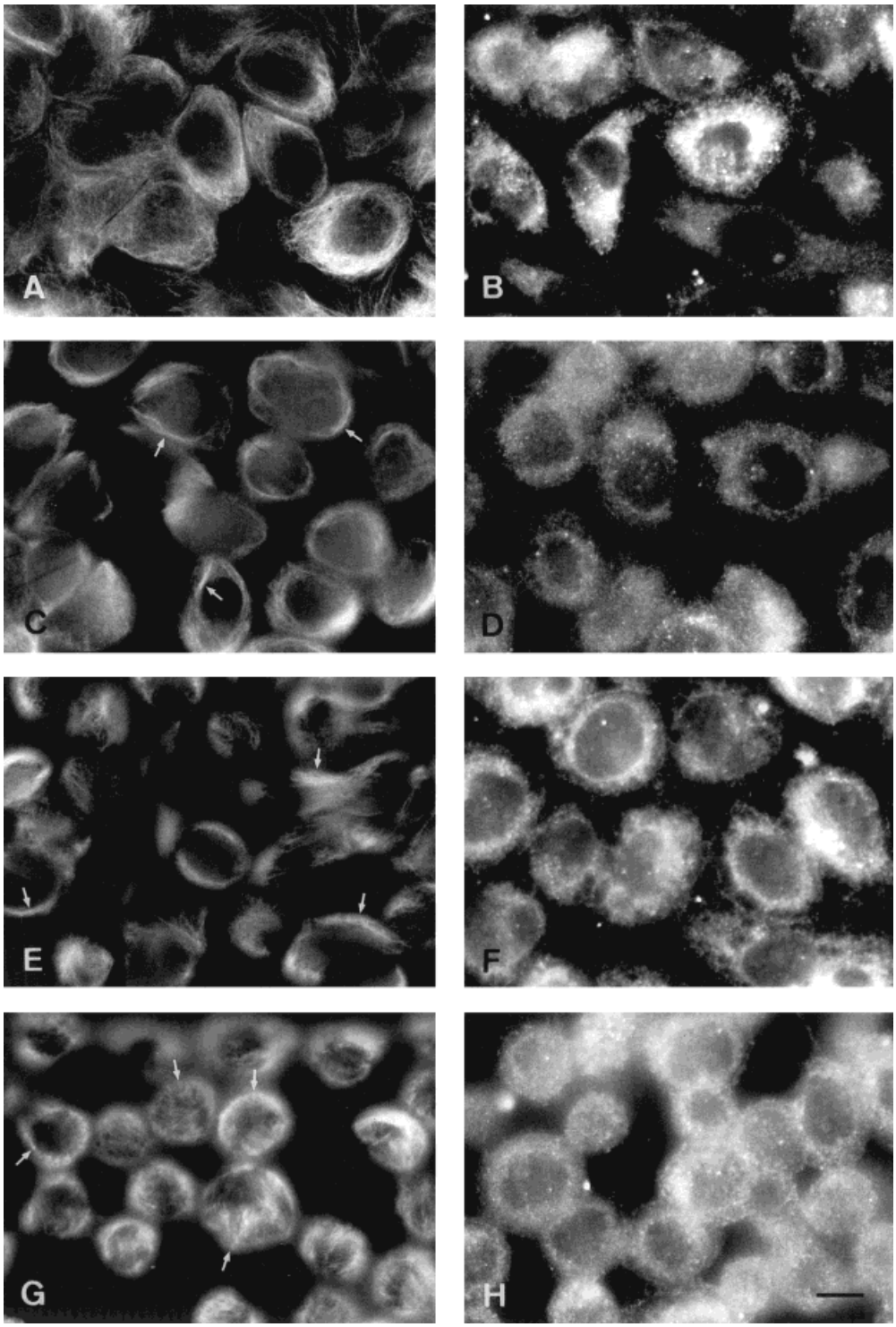

Fig. 3. Immunofluorescence staining for β-tubulin and adenomatous polyposis coli (APC) protein in control and Taxol-treated TW-039 cells. TW-039 cells were treated with 0 (**A, B**), 0.1 (**C, D**), 1 (**E, F**), or 5 (**G, H**) μM Taxol and were then fixed and immunolabeled with anti-β-tubulin (A, C, E, G) or anti-APC protein (B, D, F, H) antibodies 2 h after calcium elevation. Taxol induced bundling of the filamentous microtubules (arrows in C and E) and these bundles were disrupted into discrete segments (arrows in G) at a Taxol concentration of 5 μM. Bar = 10 μm.

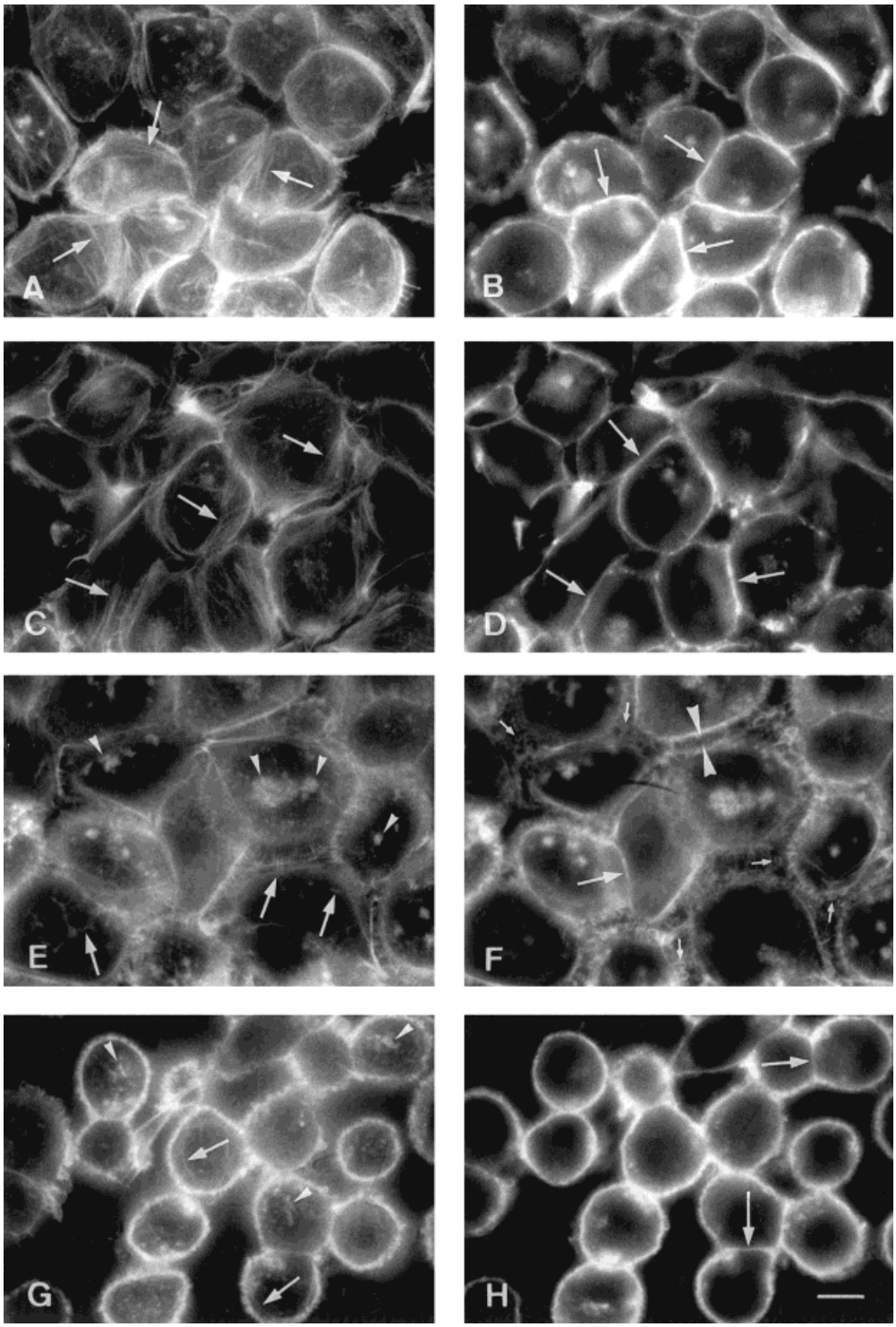

Fig. 4. Distribution of actin filaments in control and Taxol-treated TW-039 cells. TW-039 cells were treated with 0 (**A, B**), 0.1 (**C, D**), 1 (**E, F**), or 5 (**G, H**) μM of Taxol, fixed with 10% formalin, and labeled with TRITC-conjugated phalloidin 2 h after calcium elevation. Images were focused on the ventral surfaces (A, C, E, G) and the cell-cell contact sites (B, D, F, H) of confluent cells. The large arrows in A, C, E, and G indicate ventral actin filaments, and the large arrows in B, D, F, and H indicate perijunctional actin. The arrowheads in E and G indicate actin clumps. Membrane blebbing (small arrows in F) and intercellular space widening (arrowheads in F) were noted when the Taxol concentration was 1 μM. Bar = 10 μm.

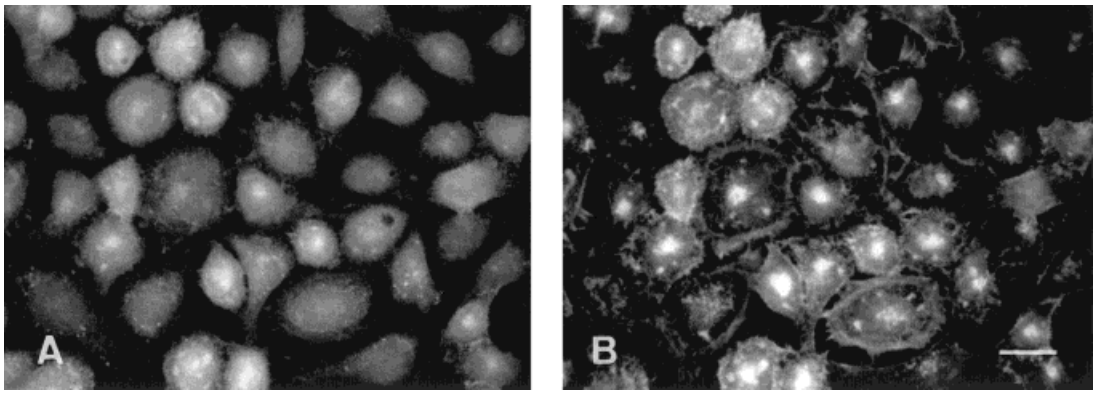

Fig. 5. Distribution of E-cadherin and actin filaments in TW-039 cells in low calcium medium (LCM). TW-039 cells were incubated in LCM for 24 h, fixed with 10% formalin, and immunolabeled with a mouse anti-E-cadherin (**A**) antibody and an FITC-conjugated goat anti-mouse IgG secondary antibody and double-labeled with TRITC-conjugated phalloidin (**B**). No junctional staining of E-cadherin was observed. Bar = 20 μm.

tant to TX-100 extraction, whereas the free cytosolic cadherins and catenins are TX-100 soluble [Pasdar and Nelson, 1988; McNeill et al., 1993]. To study quantitative changes in E-cadherin and β-catenin in these two different pools, we performed TX-100 extraction on control and Taxol-treated cells, followed by immunoblotting experiments (Fig. 7). Densitometric analysis of the TX-100-soluble pools demonstrated levels of E-cadherin and β-catenin to be, respectively, 110% and 94% of control levels in cells treated with 0.1 μM Taxol (Fig. 7A). In contrast, in cells treated with 1 or 5 μM Taxol, the level of E-cadherin fell to 53% (Bonferroni *t*-test, n = 3, $P < 0.01$) or 58% ($P < 0.01$), respectively, whereas the level of β-catenin fell to 76% ($P < 0.05$) or 74% ($P < 0.05$) (Fig. 7A). TX-100-soluble pools of α- and γ-catenin (Fig. 7A) and TX-100-insoluble pools of E-cadherin and catenins (Fig. 7B) were unchanged.

APC and GSK-3β Expression and Tyrosine Phosphorylation of β-Catenin are Unchanged After Taxol Treatment

The tumor suppressor protein, APC, is microtubule-bound and is involved in the degradation of free cytoplasmic β-catenin [Ben-Ze'ev and Geiger, 1998]. An immunoprecipitation study was therefore carried out to evaluate the association of microtubules, APC, and β-catenin. Immunoblot/densitometric analyses of β-tubulin coimmunoprecipitated with APC showed β-tubulin levels of 103%, 14% ($P < 0.01$), or 13% ($P < 0.01$), respectively, in cells treated with 0.1, 1, or 5μM Taxol. Similar tests using anti-β-catenin antibodies gave corresponding values of 101%, 9% ($P < 0.01$), or 9% ($P < 0.01$) (Fig. 8A). No E-cadherin immunoreactivity was found in APC immunoprecipitates in either control or Taxol-treated cells (data not shown). The level of APC protein was unchanged after Taxol treatment (Fig. 8B). Free cytoplasmic β-catenins can be degraded both by tyrosine or serine phosphorylation through GSK-3β [Ben-Ze'ev and Geiger, 1998]. Taxol treatment had no apparent effect on the tyrosine (arrow, Fig. 9) and serine (data not shown) phosphorylation pattern of β-catenin in TW-039 cells. Immunoprecipitation of β-catenin and subsequent probing with anti-phosphotyrosine antibodies also failed to detect tyrosine-phosphorylated β-catenin in either control or Taxol-treated cells (data not shown). GSK-3β expression was also unchanged following Taxol treatment (Fig. 9).

DISCUSSION

Taxol is an important chemotherapeutic agent used in the treatment of many types of cancers. By modulating microtubule dynamics, Taxol blocks cell-cycle progression and induces apoptosis. Because the doubling time of TW-039 cells is relatively short (about 10.5 h) [Lin et al., 1990], we focused on the short-term effects of Taxol on the E-cadherin/catenin/actin complex when the cells were not undergoing mitosis. Previous immunofluorescence microscopy studies have demonstrated that the most visible effect of Taxol on cells is the formation of microtubule bundles in interphase cells and

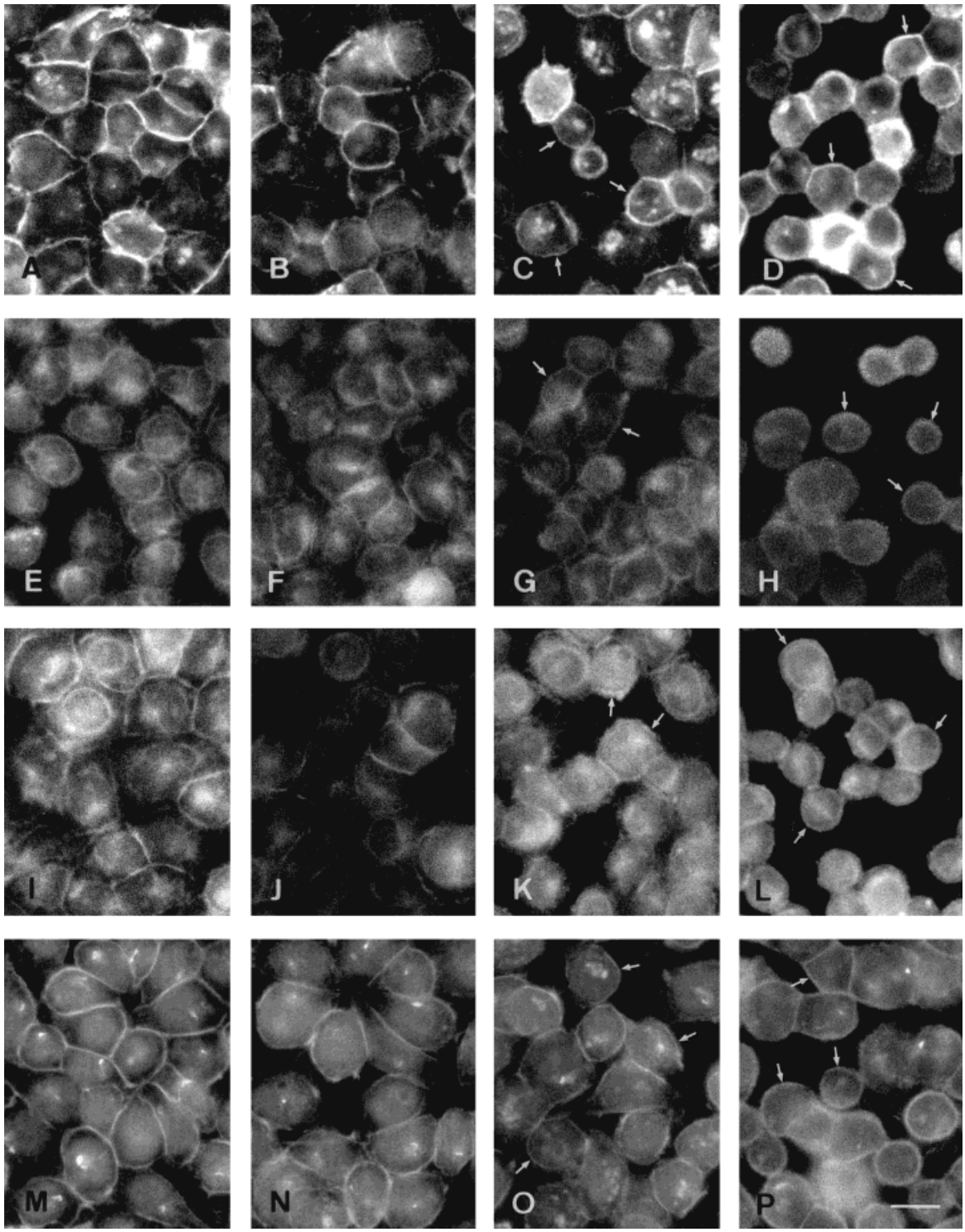

Fig. 6. Immunofluorescence staining for E-cadherin and α-, β-, or γ-catenin in control and Taxol-treated TW-039 cells. TW-039 cells were treated with 0 (**A, E, I, M**), 0.1 (**B, F, J, N**), 1 (**C, G, K, O**), and 5 (**D, H, L, P**) μM Taxol, fixed, and immunolabeled with anti-E-cadherin (**A–D**), anti-α-catenin (**E–H**), anti-β-catenin (**I–L**), or anti-γ-catenin (**M–P**) antibodies 2 h after calcium elevation. The arrows show examples of membrane staining for E-cadherin (C, D), α-catenin (G, H), β-catenin (K, L), and γ-catenin (O, P), respectively, in nonjunctional areas (not cell-cell contact sites). Bar = 20 μm.

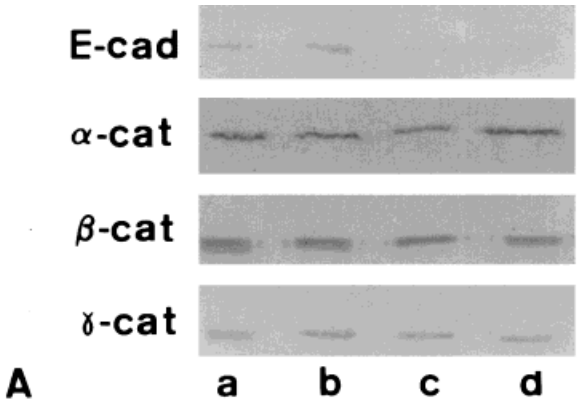

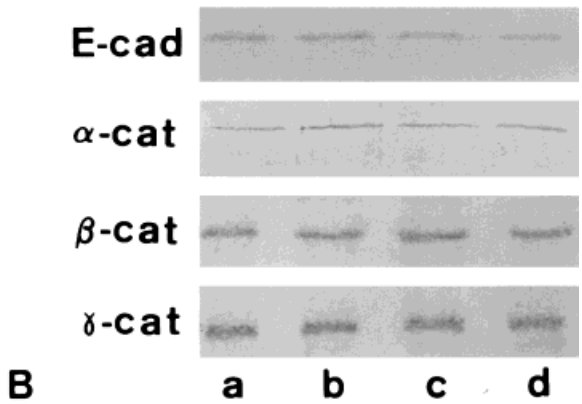

Fig. 7. Immunoblot analysis of detergent-soluble and detergent-insoluble pools of the E-cadherin/catenin complex in control and Taxol-treated TW-039 cells. TW-039 cells were treated with 0 (**lane a**), 0.1 (**lane b**), 1 (**lane c**), and 5 (**lane d**) μM Taxol and subjected to TX-100 extraction, yielding detergent-soluble (**A**) and detergent-insoluble (**B**) pools of proteins. Equivalent aliquots of each fraction were separated on gels, transblotted, and probed with antibodies specific for E-cadherin, α-, β-, or γ-catenin, as indicated.

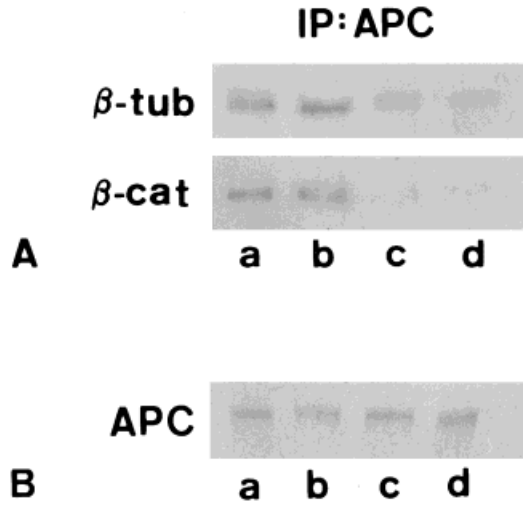

Fig. 8. Immunoblot analysis of the β-catenin/adenomatous polyposis coli (APC)/microtubule complex in control and Taxol-treated TW-039 cells. TW-039 cells were treated with 0 (**lane a**), 0.1 (**lane b**), 1 (**lane c**), and 5 (**lane d**) μM Taxol and immunoprecipitated (IP) with antibodies specific for APC (**A**). Equivalent aliquots of each fraction were separated on 10% SDS-PAGE, transblotted, and probed with antibodies specific for β-tubulin (β-tub) or β-catenin (β-cat) as indicated. **B:** Equivalent aliquots of total proteins of TW-039 cells were separated on 5% SDS-PAGE, transblotted, and probed with anti-APC protein antibodies.

spindle asters during mitosis [Manfredi and Horwitz, 1984; Garcia et al., 1994; Long and Fairchild, 1994]. In the present study, large microtubule bundles formed following treatment with either low (0.1 μM) or high (1 μM) concentrations of Taxol. Furthermore, no spindle asters were found in control or Taxol-treated TW-039 cells, confirming that, using the present experimental protocol, the cells were not entering M phase. Although the effect of Taxol on the reorganization of microtubules is both concentration- and time-dependent [Manfredi and Horwitz, 1984; Garcia et al., 1994], the mechanism by which Taxol induces microtubular bundle formation has not been fully established. The formation of microtubule bundles seen in this study in TW-039 cells treated with either low (0.1 μM) or high (1 μM) concentrations of Taxol is in good agreement with the results of previous studies [Manfredi and Horwitz, 1984; Garcia et al., 1994]. However, when an even higher concentration (5 μM) of Taxol was used, discrete segments of microtubule were observed instead of large microtubule bundles. The dramatic morphologic changes in the cells induced by the high concentration of Taxol (Fig. 2G, 2H) may be attributed to microtubule fragmentation and concomitant changes in actin filaments (Fig. 4G, 4H).

The integrity of the microtubule cytoskeleton is known to be involved in the generation of cell polarity and in membrane vesicle targeting [Grindstaff et al., 1998; Gilbert et al., 1991; Matter et al., 1990]. Many previous studies have shown microtubular involvement in protein targeting to the apical plasma membrane [Grindstaff et al., 1998; Gilbert et al., 1991;

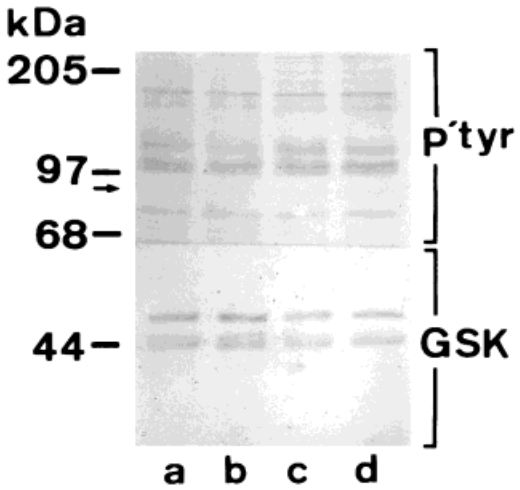

Fig. 9. Immunoblot analysis of phosphotyrosine and glycogen synthase kinase (GSK) in control and Taxol-treated TW-039 cells. TW-039 cells were treated with 0 (**lane a**), 0.1 (**lane b**), 1 (**lane c**), and 5 (**lane d**) μM Taxol. Equivalent aliquots of each fraction were separated on 10% SDS-PAGE and transblotted. The nitrocellulose membrane was cut into two pieces and the upper half probed with antibodies specific for phosphotyrosine (P'tyr) and the lower half with antibodies specific for GSK-3. The numbers on the left indicate the positions of molecular mass markers in kilodaltons. The arrow indicates the position of β-catenin.

Sauders and Limbird, 1997]. However, there is debate regarding microtubular involvement in protein delivery to the basolateral plasma membrane, the domain containing the adherens junction in epithelial cells. In MDCK cells, microtubule disruption by low temperature and nocodazole results in a ≈30% reduction in the amount of newly synthesized E-cadherin delivered to the basolateral plasma membrane [Grindstaff et al., 1998]. In cultured thymocytes, microtubule depolymerization by colchicine causes disruption of tight junctions and adherens junctions, and results in discontinuous staining for ZO-1 and E-cadherin [Yap et al., 1995]. However, other studies found microtubule disruption to have no effect on basolateral plasma membrane protein delivery [Gilbert et al., 1991; Sauders and Limbird, 1997]. Our immunofluorescence microscopy study showed that although Taxol (1 or 5 μM) induced TW-039 cells to separate from one another, circular staining for E-cadherin and catenins was still seen at the cell membrane. This staining pattern coincided with the actin staining pattern in Taxol-treated cells (Fig. 4F, 4H). In individual motile cells, actin filaments are continually polymerized at the free cell edge of the cell lamellae and depolymerized in a transition zone between the cell body and lamellae [Adams et al., 1998]. This transition zone is characterized by a conspicuous continuous ring of actin, called the circumferential actin cable, which is associated with the adherens junction of polarized epithelial cells [Hirano et al., 1987; Adams et al., 1998]. Because E-cadherin and the catenins are linked to the actin-based cytoskeleton [Tsukita et al., 1992], the circular staining pattern of E-cadherin and the catenins seen in the present study may represent the complex formed between these intercellular junctional proteins and the circumferential actin cables. Taken together, these results suggest that the modulation of microtubule dynamics by Taxol did not affect the formation of the E-cadherin/catenin/actin complex at the adherens junction of TW-039 cells.

The cadherin/catenin/actin complex at the cell-cell junction is resistant to TX-100 extraction, whereas the free cytosolic cadherin and catenins are TX-100 soluble [Pasdar and Nelson, 1988; McNeill et al., 1993]. In the present study, immunoblot/densitometric analyses showed that levels of the TX-100-insoluble pools of E-cadherin and the catenins were unchanged following Taxol treatment, supporting the immunostaining findings that the formation of the E-cadherin/catenin/actin complex is unaffected by Taxol using the present experimental protocol. In contrast, following treatment with Taxol at concentrations of 1 or 5 μM, levels of the TX-100-soluble pools of E-cadherin and β-catenin were, respectively, reduced by 47% and 24% in cells treated with 1 μM Taxol, and by 42% and 26% in cells treated with 5 μM Taxol. These results indicate that, at high concentrations (1 or 5 μM), Taxol causes ≈45% reduction in cytosolic E-cadherin and 25% reduction in cytosolic β-catenin, an E-cadherin/β-catenin reduction ratio of about 1.8:1. This agrees with the results of a previous study by Hinck and colleagues [1994] on the stoichiometry of the cadherin/catenin complex that demonstrated the molecular ratio of E-cadherin:β-catenin in the TX-100-soluble fraction, with or without chemical cross-linking, to be 1:0.5. The question then arises why levels of α- and γ-catenin are not affected by Taxol. In the same study, Hinck and colleagues [1994] showed that, immediately after synthesis, the cadherin/β-catenin and cadherin/γ-catenin complexes are found in the TX-100-soluble fraction. In contrast,

α-catenin does not associate with the E-cadherin/β-catenin until the complex reaches the cell membrane, and so is found in the TX-100-insoluble fraction [Hinck et al., 1994]. If the effect of Taxol is on the assembly or degradation of the cadherin/catenin complex in the cytosol, α-catenin may therefore not be affected, since it is not part of the cytosolic cadherin/catenin complex. In addition, because only a small proportion of the γ-catenin is associated with E-cadherin in the TX-100-soluble fraction [Hinck et al., 1994], any effects of Taxol on the cytosolic cadherin/catenin complex may be too small to influence the level of γ-catenin. However, we cannot exclude the possibility that the expression of E-cadherin and β-catenin may be selectively regulated at high Taxol concentrations.

Homeostasis between the E-cadherin/catenin/actin and β-catenin/APC/GSK-3β complexes is the key regulator of cellular levels of E-cadherin and β-catenin [Ilyas and Tomlinson, 1997; Ben-Ze'ev and Geiger, 1998]. Formation of the β-catenin/APC/GSK-3β complex results in the subsequent proteolytic degradation of β-catenin. Because APC protein is closely associated with the microtubules, and because Taxol modulates the dynamics of, and results in dramatic morphological changes in, microtubules, it is reasonable to speculate that the expression of APC protein or its binding to β-catenin may also be affected. Immunofluorescence microscopy and immunoblot analyses showed that neither the staining pattern (Fig. 3B, 3D, 3F, 3H) nor the expression levels of APC (Fig. 8B) were altered following Taxol treatment. If the observed reduction in cytosolic β-catenin occurs through association with APC protein and subsequent degradation, one would anticipate an increased binding of APC protein and β-catenin at high concentrations of Taxol. However, immunoprecipitation and immunoblot analyses showed that the binding of APC protein to both β-tubulin and β-catenin was decreased by treatment with high concentrations of Taxol (Fig. 8A). It has also been reported that activation of GSK-3β may phosphorylate APC protein, thus enhancing its efficiency for degrading β-catenin [Rubinfeld et al., 1996; Ilyas and Tomlinson, 1997]. In the present study, levels of GSK-3β (Fig. 9, lower panel) and its phosphorylation pattern (data not shown) were both unchanged in TW-039 cells. The serine phosphorylation pattern of β-catenin was also unchanged (data not shown). In addition to phosphorylation at serine or threonine residues, phosphorylation of β-catenin at tyrosine residues can also regulate the expression and function of the cadherin/catenin complex [reviewed in Daniel and Reynolds, 1997]. However, in the present study, the tyrosine phosphorylation pattern of cells was also unchanged following Taxol treatment (Fig. 9, upper panel). Our results imply that, in TW-039 cells, modulation of microtubule dynamics by Taxol reduces the cytosolic E-cadherin and β-catenin through pathways not involving β-catenin phosphorylation.

The mechanism by which Taxol induces morphologic changes in the actin cytoskeleton is also intriguing. Historically, actin filaments and microtubule arrays have been viewed as constituting separate cytoskeletal systems. However, a growing number of observations show that these two filament systems may be closely associated. For example, the identification of microtubule actin cross-linking factors [Leung et al., 1999] and microtubule-bound small G-proteins [Hotta et al., 1996; Tian et al., 2000; Best et al., 1996] may provide a functional link between these two filament systems. Ren and colleagues [1998] have reported that GEF-H1, a member of the Dbl family, colocalizes with microtubules through the carboxyl-terminal coiled-coil domain and that overexpression of GEF-H1 in COS-7 cells results in Rac activation and subsequent reorganization of the actin filaments. Another study on the Dbl-related protein, Lfc, by Glaven and colleagues [1999] showed that the pleckstrin homology domain-mediated localization of Lfc to microtubules enables the recruitment of Rac to its signaling targets, resulting in c-Jun kinase activation and actin cytoskeletal changes. Based on these observations, a possible mechanism for the morphologic changes in the actin cytoskeleton seen in the present study may be through the effects of Taxol on the cross-linking factors and/or these small G-proteins. Further studies are needed to examine this question.

In this study, we have shown that high concentrations of Taxol affect the actin cytoskeleton and reduce levels of cytosolic E-cadherin and β-catenin in TW-039 cells. In contrast, the formation of the E-cadherin/catenin/actin complex at the adherens junction in these cells is not affected by Taxol. Although the effects of Taxol on cells are not fully understood, our study demonstrated a cross-talk between the microtubule- and actin-based cytoskeletal com-

partments. The mechanism by which Taxol induces morphologic changes in actin filaments is still unclear and further studies on Taxol-related effects on microtubule-actin cross-linking proteins and small G-proteins will be key steps in elucidating this point.

ACKNOWLEDGMENTS

We thank Dr. Seu-Mei Wang for helpful discussion. Mouse monoclonal antibody against β-tubulin, developed by Dr. Michael Klymkowsky, was obtained from the Developmental Studies Hybridoma Bank maintained by the University of Iowa, Department of Biological Science, Iowa City, IA, under contract NO1-HD-7-3263 from the NICHD.

REFERENCES

Adams CL, Chen YT, Smith SJ, Nelson WJ. 1998. Mechanism of epithelial cell-cell adhesion and cell compaction revealed by high-resolution tracking of E-cadherin-green fluorescence protein. J Cell Biol 142: 1105–1119.

Ben-Ze'ev A, Geiger B. 1998. Differential molecular interactions of β-catenin and plakoglobin in adhesion, signaling and cancer. Curr Opin Cell Biol 10:629–639.

Best A, Ahmed S, Kozma R, Lim L. 1996. The Ras-related GTPase Rac1 binds tubulin. J Biol Chem 271:3756–3762.

Carmichael J, DeGraff WG, Gazdar AF, Minna JD, Mitchell JB. 1987. Evaluation of a tetrazolium-based semiautomated colorimetric assay: assessment of chemosensitivity testing. Cancer Res 47:936–942.

Daniel JM, Reynolds AB. 1997. Tyrosine phosphorylation and cadherin/catenin function. BioEssays 19:883–891.

Garcia P, Braguer D, Carles G, el Khyari S, Barra Y, de Ines C, Barasoain I, Briand C. 1994. Comparative effects of Taxol and taxotere on two different human carcinoma cell lines. Cancer Chemother Pharmocol 34:335–343.

Gilbert T, Le Bivic A, Quaroni A, Rodriguez-Boulan E. 1991. Microtubule organization and its involvement in the biogenetic pathways of plasma membrane proteins in Caco-2 intestinal epithelial cells. J Cell Biol 113:275–288.

Glaven JA, Whitehead I, Bagrodia S, Kay R, Cerione RA. 1999. The Dbl-related protein, Lfc, localizes to microtubules and mediates the activation of Rac signaling pathways in cells. J Biol Chem 274:2279–2285.

Grindstaff KK, Bacallao RL, Nelson WJ. 1998. Apiconuclear organization of microtubules does not specify protein delivery from the trans-Golgi network to different membrane domains in polarized epithelial cells. Mol Biol Cell 9:685–699.

Hinck L, Nathke IS, Papkoff J, Nelson WJ. 1994. Dynamics of cadherin/catenin complex formation: novel protein interactions and pathways of complex assembly. J Cell Biol 125:1327–1340.

Hirano S, Hose A, Hatta K, Kawakami A, Takeichi M. 1987. Calcium-dependent cell-cell adhesion molecules (cadherins): subclass specificities and possible involvement of actin bundles. J Cell Biol 105:2501–2510.

Hotta K, Tanaka K, Mino A, Kohno H, Takai Y. 1996. Interaction of the Rho family small G proteins with kinectin, an anchoring protein of kinesin motor. Biochem Biophys Res Commun 225:69–74.

Ilyas M, Tomlinson IPM. 1997. The interactions of APC, E-cadherin and β-catenin in tumor development and progression. J Pathol 182:128–137.

Jordan MA, Wendell KL, Gardiner S, Derry WB, Copp H, Wilson L. 1996. Mitotic block induced in HeLa cells by low concentrations of paclitaxel (Taxol) results in abnormal mitotic exit and apoptotic cell death. Cancer Res 56:816–825.

Jordan MA, Wilson L. 1998. Microtubules and actin filaments: dynamic targets for cancer chemotherapy. Curr Opin Cell Biol 10:123–130.

Leung CL, Sun D, Zheng M, Knowles DR, Liem RKH. 1999. Microtubule actin cross-linking factor (MACF): a hybrid of dystonin and dystrophin that can interact with the actin and microtubule cytoskeletons. J Cell Biol 147: 1275–1285.

Lin CT, Wong CI, Chan WY, Chan WY, Tzung KW, Ho JKC, Hsu MM, Chuang SM. 1990. Establishment and characterization of two nasopharyngeal carcinoma cell lines. Lab Invest 62:713–724.

Long BH, Fairchild CR. 1994. Paclitaxel inhibits progression of mitotic cells to G1 phase by interference with spindle formation without affecting other microtubule functions during anaphase and telephase. Cancer Res 54:4355–4361.

Lou PJ, Chen WP, Lin CT, DePhilip RM, Wu JC. 2000. E-, P-, and N-cadherin are co-expressed in the nasopharyngeal carcinoma cell line TW-039. J Cell Biochem 76:161–172.

Manfredi JJ, Horwitz SB. 1984. Taxol: an antimitotic agent with a new mechanism of action. Pharmocol Ther 25:83–125.

Mareel M, Boterberg T, Noe V, Van Hoorde L, Vermeulen S, Bruyneel E, Bracke M. 1997. E-cadherin/catenin/cytoskeleton complex: a regulator of cancer invasion. J Cell Physiol 173:271–274.

Matter K, Bucher K, Hauri HP. 1990. Microtubule perturbation retards both the direct and the indirect apical pathway but does not affect sorting of plasma membrane proteins in intestinal epithelial cells (Caco-2). EMBO J 9:3163–3170.

McNeill H, Ryan TA, Smith SJ, Nelson WJ. 1993. Spatial and temporal dissection of immediate and early events following cadherin-mediated epithelial cell adhesion. J Cell Biol 120:1217–1226.

Nathke IS, Adams CL, Polakis P, Sellin JH, Nelson WJ. 1996. The adenomatous polyposis coli tumor suppressor protein localizes to plasma membrane sites involved in active cell migration. J Cell Biol 134:165–179.

Pasdar M, Nelson WJ. 1988. Kinetics of desmosome assembly in Madin-Darby canine kidney epithelial cells: temporal and spatial regulation of desmoplakin organization and stabilization upon cell-cell contact. I. Biochemical analysis. J Cell Biol 106:677–685.

Ren Y, Li R, Zheng Y, Busch H. 1998. Cloning and characterization of GEF-H1, a microtubule-associated guanine nucleotide exchange factor for Rac and Rho GTPases. J Biol Chem 273:34954–34960.

Rubinfeld B, Albert I, Porfiri E, Fiol C, Munemitsu S, Polakis P. 1996. Binding of GSK3β to the APC-β-catenin complex and regulation of complex assembly. Science 272:1023–1026.

Sauders C, Limbird LE. 1997. Disruption of microtubules reveals two independent apical targeting mechanisms for G-protein-coupled receptors in polarized renal epithelial cells. J Biol Chem 272:19035–19045.

Schief PB, Fant J, Horwitz SB. 1979. Promotion of microtubule assembly in vitro by Taxol. Nature 277:665–667.

Takeichi M. 1991. Cadherin cell adhesion receptors as a morphogenetic regulator. Science 251:1451–1455.

Tian L, Nelson DL, Stewart DM. 2000. Cdc42-interacting protein 4 mediates binding of the Wiskott-Aldrich syndrome protein to microtubules. J Biol Chem 275:7854–7861.

Trielli M, Andreasson PR, Lacroix FB, Margolis RL. 1996. Differential Taxol-dependent arrest of transformed and nontransformed cells in the G1 phase of the cell cycle, and specific-related mortality of transformed cells. J Cell Biol 135:689–700.

Tsukita SH, Tsukita SA, Nagafuchi A, Yonemura S. 1992. Molecular linkage between cadherins and actin filaments in cell-cell adherens junctions. Curr Opin Cell Biol 4:834–839.

Twentyman PR, Luscombe M. 1987. A study of some variables in a tetrazolium dye (MTT) based assay for cell growth and chemosensitivity. Br J Cancer 56:279–285.

Woods CM, Zhu J, McQueney PA, Bollag D, Lazarides E. 1995. Taxol-induced mitotic block triggers rapid onset of a P53-independent apoptotic pathway. Mol Med 1:1076–1551.

Yap AS, Stevenson BR, Abel KC, Cragoe EJ, Manley SW. 1995. Microtubule integrity is necessary for the epithelial barrier function of cultured thyroid cell monolayers. Exp Cell Res 218:540–550.